Research Article

Characterization of bacteriophage BUCT631 lytic for K1 *Klebsiella pneumoniae* and its therapeutic efficacy in *Galleria mellonella* larvae

Pengjun Han [a], Mingfang Pu [a], Yahao Li [b], Huahao Fan [a,*], Yigang Tong [a,b,*]

[a] *College of Life Science and Technology, Beijing University of Chemical Technology, Beijing, 100029, China*
[b] *Beijing Advanced Innovation Center for Soft Matter Science and Engineering, Beijing University of Chemical Technology, Beijing, 100029, China*

ARTICLE INFO

ABSTRACT

Severe infections caused by multidrug-resistant *Klebsiella pneumoniae* (*K. pneumoniae*) highlight the need for new therapeutics with activity against this pathogen. Phage therapy is an alternative treatment approach for multidrug-resistant *K. pneumoniae* infections. Here, we report a novel bacteriophage (phage) BUCT631 that can specifically lyse capsule-type K1 *K. pneumoniae*. Physiological characterization revealed that phage BUCT631 could rapidly adsorb to the surface of *K. pneumoniae* and form an obvious halo ring, and it had relatively favorable thermal stability (4–50 °C) and pH tolerance (pH = 4–12). In addition, the optimal multiplicity of infection (MOI) of phage BUCT631 was 0.01, and the burst size was approximately 303 PFU/cell. Genomic analysis showed that phage BUCT631 has double-stranded DNA (total length of 44,812 bp) with a G + C content of 54.1%, and the genome contains 57 open reading frames (ORFs) and no virulence or antibiotic resistance related genes. Based on phylogenetic analysis, phage BUCT631 could be assigned to a new species in the genus *Drulisvirus* of the subfamily *Slopekvirinae*. In addition, phage BUCT631 could quickly inhibit the growth of *K. pneumoniae* within 2 h *in vitro* and significantly elevated the survival rate of *K. pneumoniae* infected *Galleria mellonella* larvae from 10% to 90% *in vivo*. These studies suggest that phage BUCT631 has promising potential for development as a safe alternative for control and treatment of multidrug-resistant *K. pneumoniae* infection.

1. Introduction

Klebsiella pneumoniae (*K. pneumoniae*), as a clinically common gram-negative bacillus of the *Enterobacteriaceae* family, is an important opportunistic pathogen causing pulmonary infections, urinary tract infections and sepsis (Podschun and Ullmann, 1998). *K. pneumoniae* has two main pathotypes: hypervirulent *K. pneumoniae* (hvKp) and classical *K. pneumoniae* (cKp). The capsule is one of the most important virulence factors of *K. pneumoniae*. Among more than 80 types of capsule serotypes, K1, K2, K5, K20, K54 and K57 are closely related to various invasive infections in humans, among which K1 is the most virulent and most common (Chuang et al., 2006). In contrast to cKp, K1 *K. pneumoniae* (a predominant sequence type of hvKp) causes a distinctive syndrome of community-acquired pyogenic liver abscess that is complicated by metastatic endophthalmitis or central nervous system (CNS) infections even in healthy individuals (Choby et al., 2020; Fang et al., 2007). Recently, K1 *K. pneumoniae* has emerged in China and other Asian countries, and poses great challenges for clinical treatment (Harada et al., 2018; Zhang et al., 2016).

Antibiotics have long been considered as the most powerful weapon in the treatment of bacterial infectious diseases, and carbapenems are the first-line antibiotics for the treatment of *K. pneumoniae* infections (Thapa et al., 2021). However, the protracted irrational employment of antibiotics has led to the proliferation and dissemination of multidrug-resistant *K. pneumoniae*, impeding efficacious treatment of both nosocomial and community-acquired infections, and engendering a grave menace to vulnerable patient populations (Bengoechea and Sa Pessoa, 2019; Ramirez et al., 2014). Significantly, antibiotic resistance in K1 *K. pneumoniae* strains is increasing and the mortality rate in patients infected with these strains is high (Lin et al., 2018). Therefore, there is an urgent need for new antibiotic alternatives to treat infections caused by multidrug-resistant K1 *K. pneumoniae*.

Bacteriophages (or phages), the viruses that specifically infect and lyse bacteria, are widely distributed in nature, and have been used to treat bacterial infections since their discovery (Wittebole et al., 2014). Unlike the bactericidal mechanism of antibiotics, phages infect bacteria by recognizing bacterial surface receptors (Letarov and Kulikov, 2017) and thus are not limited by bacterial drug resistance. Phages also have

---

* Corresponding authors.
E-mail addresses: fanhuahao@mail.buct.edu.cn (H. Fan), tongyigang@mail.buct.edu.cn (Y. Tong).

the advantages of low cost and high safety (Luong et al., 2020; Sarker et al., 2012), and are gradually becoming a major topic for the development of antibacterial agents. Significant progress has been made in the prevention and treatment of bacterial infections using natural or modified virulent phages, and phages have been successfully used to treat oral, pulmonary, genital, intestinal, cardiac, and skin infections (Melo et al., 2020). Notably, phages have also shown encouraging therapeutic efficacy in the clinical treatment of severe infections caused by multi-drug-resistant *K. pneumoniae* (Bao et al., 2020; Cano et al., 2021). Thus, phages would be ideal candidates for the treatment of multidrug-resistant *K. pneumoniae* infections.

Bacteriophages are remarkably specific to their host bacteria and only replicate in the presence of bacteria causing the infection. This specificity of phages prevents negative impacts on the patient microbiome and avoids driving the resistance of nontarget species (Saha and Mukherjee, 2019), which makes them safe for therapy. However, this specificity allows phages to have a narrow host range, and becomes a factor limiting the widespread use of phages. The discovery of new phages and the evaluation of their antimicrobial capacity, along with their preparation into phage cocktails, is an effective way to overcome these limitations (Hatfull et al., 2022). In addition, analysis of the phage genome to ensure the absence of virulence and resistance genes is a necessary prerequisite for phage therapy (McCallin et al., 2013).

Phages of *K. pneumoniae* have been isolated from a variety of sources around the world, including wastewater, sewage, seawater, and human intestinal samples (Herridge et al., 2020; Li et al., 2022a). However, this is only the tip of the iceberg and there are still a large number of un-discovered phages. Isolation and characterization of novel *K. pneumoniae* phages are essential to further expand our understanding of *K. pneumoniae* phage diversity, evolution, and phage-host interactions. In this study, we isolated a *K. pneumoniae* phage, named BUCT631, from hospital sewage samples. Biological characteristic investigation, whole genome sequence analysis, and evaluation of therapeutic efficacy *in vitro* and *in vivo* were performed to provide a comprehensive understanding of the antibacterial potential of BUCT631. Our study lays the foundation for the application of phage BUCT631 as an alternative to antibiotics in future clinical treatments.

2. Materials and methods

2.1. Bacterial strains and culture conditions

All *K. pneumoniae* strains used in this study were isolated from environmental samples of Aviation General Hospital and 307 Hospital, Beijing, China, and stored at $-80\ ^\circ$C in our laboratory with 50% glycerol (v/v). The multilocus sequence typing and capsule type of strains were identified in our previous studies (Pu et al., 2022). The antibiotic sensitivity test results of K1 *K. pneumoniae* are shown in Supplementary Table S1. All strains were cultivated in Luria-Bertani (LB) broth at 37 $^\circ$C with shaking (220 rpm). Bacterial clone isolation and counting were performed using LB solid medium (1.5% w/v agar).

2.2. Phage BUCT631 isolation and purification

Phage BUCT631 was isolated from sewage collected in Aviation General Hospital using *K. pneumoniae* strain K7 as previously described with slight modifications (Han et al., 2021). Briefly, sewage samples were centrifuged at 12,000 $\times g$ for 5 min, and the supernatant was filtered using a 0.22 μm filter unit (Pall, USA). The filtrate was then incubated with strain K7 in LB liquid at 37 $^\circ$C with shaking (220 rpm) for 24 h. The mixed culture solution was centrifuged at 12,000 $\times g$ for 5 min, and the supernatant was filtered using a 0.22 μm filter unit. The single plaque was isolated using a soft agar overlay with the mixture of supernatant and strain K7. Purification of phage BUCT631 was performed using the cesium chloride density gradient centrifugation method as previously described (Han et al., 2022).

2.3. Electron microscopy

For electron microscopy, phage stocks were prepared as described above, and 30 μL of phage lysate was incubated with a carbon-coated copper grid for 10 min, stained with 2% uranyl acetate for 90 s and subsequently air dried. The morphology of the phages was observed using a transmission electron microscope (JEM-1200EX, JEOL, Tokyo, Japan) at 80 kV.

2.4. Host range

Host range analysis was performed using a panel of thirty *K. pneumoniae* strains by spot tests as previously described with slight modifications (Kim et al., 2020). Briefly, the purified phage stocks were gradient diluted with phosphate buffer saline (PBS), and 2 μL of gradient diluted phage concentrate (10^3–10^9 PFU/mL) was added to the tested bacterial lawn and incubated at 37 $^\circ$C for 12 h. The presence of clear plaque on the bacterial lawn indicated that the tested strains were susceptible to the phage. Moreover, susceptibility of the tested strain to the phage BUCT631 was also performed using the efficiency of plaquing (EOP) method (Holst Sørensen et al., 2012). Plaque formation on *K. pneumoniae* strain K7 served as a reference for EOP calculation.

2.5. Optimal multiplicity of infection

To determine the optimal multiplicity of infection (MOI), 100 μL of K7 culture (2×10^7 CFU/mL) in pre-logarithmic growth phase was mixed with different dilutions of phage suspensions at MOIs of 0.001, 0.01, 0.1, 1, 10, and 100. The mixture was then added to 5 mL of fresh LB liquid and incubated at 37 $^\circ$C with shaking (220 rpm) for 12 h. The culture medium was centrifuged at 12,000$\times g$ for 5 min, and the supernatant was filtered using a 0.22 μm filter unit to obtain the phage proliferation solution. Finally, the phage titer under different MOI conditions was determined using a soft agar overlay method (Li and Zhang, 2014), and the highest phage titer was the optimal MOI. Each group of experiments was performed in triplicate.

2.6. Adsorption assay and one-step growth curve

Adsorption experiments were carried out as previously described with some modifications (Storms and Sauvageau, 2014). In brief, *K. pneumoniae* strain K7 was cultured to logarithmic stage (approximately 1×10^8 CFU/mL), and then 1 mL of phage suspension was added to the culture medium at a final MOI of 0.01. The mixture was incubated at 37 $^\circ$C, and 200 μL of medium was collected at 0, 5, 10, 15, 20, 25 and 30 min and centrifuged at 12,000 $\times g$ for 2 min. Then, 100 μL of the supernatant was diluted with a PBS gradient, and the titer of unadsorbed phage was determined in three experiments parallel using the soft agar overlay method. Adsorption data are presented as a decrease in the free phage fraction, defined as the titer of free phage divided by the titer of initial phage.

To understand the growth pattern of phage BUCT631, a one-step growth curve was performed. *K. pneumoniae* strain K7 was cultured to logarithmic stage and mixed with phage BUCT631 at an MOI of 0.01. The mixture was incubated at 37 $^\circ$C for 15 min to allow sufficient adsorption of the phage to the bacteria and then centrifuged at 12,000 $\times g$ for 2 min to collect the bacteria. The bacteria were then washed twice with PBS and resuspended in 20 mL of fresh LB medium, and the cultures were incubated at 37 $^\circ$C with shaking (220 rpm). The 200 μL cultures were collected at 0, 10, 12, 14, 16, 18, 20, 30, 40, 50, 60, 70, 80, 90, 100, 110 and 120 min, and centrifuged at 12,000 $\times g$ for 2 min. Then, 100 μL of supernatant was used to detect phage titer in three parallel experiments using a soft agar overlay method. One-step growth curve was drawn by taking infection time as the abscissa and phage titer as the ordinate.
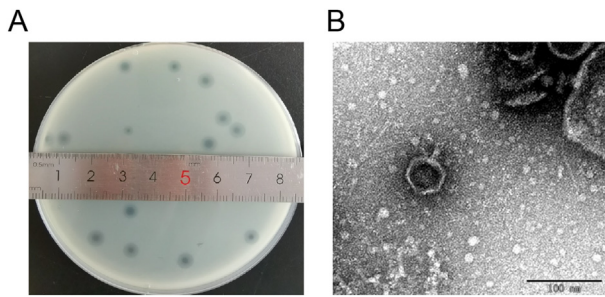
Fig. 1. Morphological observation of phage BUCT631. **A** Phage plaques formed on the lawn of *K. pneumoniae* strain K7 at 37 °C for 18 h. **B** Transmission electron micrograph of the phage.

2.7. Thermal and pH stability

The purified phage BUCT631 suspensions were incubated for 12 h at 4, 25, 37, 45, 55, 65 and 75 °C for thermal stability tests. To determine the stability of phage BUCT631 in different pH environments, the phage suspension was incubated in LB broth at different pH levels ranging from 2 to 13 for 12 h. Phage suspensions incubated at different temperatures or pH conditions were used to determine phage titer using a soft agar overlay method. Each group of experiments was performed in triplicate.

2.8. Phage DNA isolation and sequencing

The genomic DNA of phage BUCT631 was extracted using the E.Z.N.A Viral DNA Kit (Omega, Norcross, Georgia, USA) following the manufacturer's instructions. Then, a paired-end 150 bp DNA library was constructed using the NEBNext Ultra II FS DNA Library Prep Kit (NEB, USA) according to the manufacturer's instructions, and BUCT603B1 genome was sequenced on the Illumina NovaSeq 6000 platform. The raw

sequencing data were filtered for low quality reads and adapters using Trimmomatic 0.36 with default parameters (Bolger et al., 2014). Finally, the clean reads were assembled to form a 44,812 bp contig using SPAdes v3.13.0 software (Bankevich et al., 2012).

2.9. Bioinformatics analysis

Open reading frames (ORFs) were predicted using PHANOTATE (McNair et al., 2019). The ORFs were annotated using the protein basic local alignment search tool (BLASTp) of the National Center for Biotechnology Information (NCBI) server with the non-redundant (nr) sequence database (Altschul et al., 1997). Conserved domain searches were performed using CD-Search with the CDD v3.20-59693 PSSMs database (Marchler-Bauer et al., 2011). Theoretical molecular weight of the proteins was identified using Expasy ProtParam tool (Wilkins et al., 1999). The putative transfer RNA genes in the BUCT631 genome were identified with tRNAscan-SE v.2.0 (Lowe and Eddy, 1997). The possible virulence and pathogen genes carried by phage genome were predicted with the VirulenceFinder (Clausen et al., 2018) and PathogenFinder (Cosentino et al., 2013), respectively. Phage homology calculations were performed using VIRIDIC (Moraru et al., 2020). To determine the taxonomy of the phage BUCT631, phylogenetic analyses based on the DNA polymerase, terminase large subunit and major capsid were performed with MEGA7 by the neighbor-joining method and detected by the bootstrap method with 1000 test repetitions (Kumar et al., 2016).

2.10. Antibacterial activity of phage BUCT631 against K. pneumoniae strain K7 in vitro

Single colonies of *K. pneumoniae* strain K7 were picked separately into 5 mL of fresh LB culture medium and incubated at 37 °C with shaking (220 rpm) until early logarithm (OD_{600} = 0.2–0.3). Then, different dilutions of phage suspensions (10^4–10^9 PFU/mL) were added to adjust the

Table 1
Host range analysis of phage BUCT631 against thirty strains.

Species	Strains	ST type	Capsular type	Susceptibility	Origin	EOP[a]
Klebsiella pneumoniae	K7	ST23	K1	++++	Aviation General Hospital	100
	064	ST23	K1	+++	Aviation General Hospital	12
	081	ST23	K1	++	Aviation General Hospital	1.4
	2024	ST23	K1	+++	Aviation General Hospital	17
	2752	ST23	K1	+++	Aviation General Hospital	13
	2755	ST23	K1	++++	Aviation General Hospital	103
	S-2007	ST23	K1	++++	Aviation General Hospital	89
	1301	ST65	K2	–	307 Hospital	0
	1307	ST65	K2	–	307 Hospital	0
	1241	ST11	K15	–	307 Hospital	0
	1291	ST11	K27	–	307 Hospital	0
	1300	ST11	K16	–	307 Hospital	0
	2004	ST11	K47	–	Aviation General Hospital	0
	2005	ST11	K25	–	Aviation General Hospital	0
	2006	ST11	K47	–	Aviation General Hospital	0
	2008	ST11	K64		Aviation General Hospital	0
	2009	ST11	K64	–	Aviation General Hospital	0
	2012	ST11	K25	–	Aviation General Hospital	0
	2015	ST11	K47	–	Aviation General Hospital	0
	2022	ST11	K47	–	Aviation General Hospital	0
	2026	ST11	K64	–	Aviation General Hospital	0
	2086	ST11	K64	–	Aviation General Hospital	0
	2002	ST15	K19	–	Aviation General Hospital	0
	2003	ST15	K19	–	Aviation General Hospital	0
	2013	ST15	K19	–	Aviation General Hospital	0
	2017	ST15	K19	–	Aviation General Hospital	0
	2027	ST15	K19	–	Aviation General Hospital	0
	2068	ST15	K19	–	Aviation General Hospital	0
	1299	ST723	N/A	–	307 Hospital	0
	K1119	ST893	N/A	–	307 Hospital	0

++++, plaques at 10^{-6}; +++, plaques at 10^{-5}; ++, plaques at 10^{-4}; –, no plaques.
[a] EOP (efficiency of plaquing) is calculated in percent as the PFU/mL of the phages on the test strain divided by the PFU/mL obtained on strain K7 multiplied by 100.
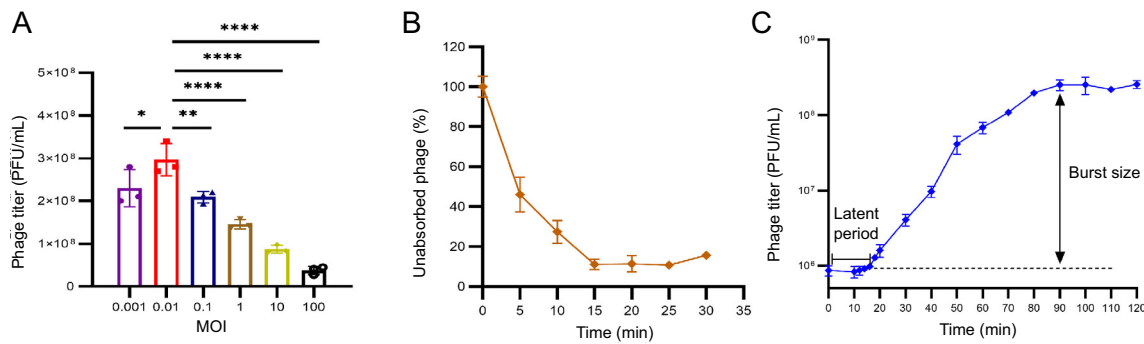
Fig. 2. Biological characterization of phage BUCT631. **A** Determination of optimal multiplicity of infection (MOI). BUCT631 was mixed with K7 at different MOIs and incubated at 37 °C for 12 h with shaking, and the phage titer was detected. **B** Adsorption curve of phage BUCT631. BUCT631 was mixed with K7 at an MOI of 0.01, and the mixture was collected at different times to detect phage titers. **C** One-step growth curve of phage BUCT631. BUCT631 was mixed with K7 at an MOI of 0.01 and incubated for 15 min, then the mixture was cultured at 37 °C with shaking and sampled for phage titer at different times. Data are shown as the mean ± standard deviation. Statistical analysis was performed by one-way analysis of variance following a Dunnett's multiple comparisons test. *$P < 0.05$, **$P < 0.01$ and ****$P < 0.0001$.

MOI to 0.001, 0.01, 0.1, 1, 10 and 100, and the mixture was incubated at 37 °C with shaking (220 rpm) for 12 h. *K. pneumoniae* strain K7 culture without phage addition was used as a control group. The absorbance (OD_{600}) of each group was measured every 1 h during the cultivation period using NanoDrop one (Thermo, USA). In addition, 100 μL samples were taken from each group every 2 h for bacterial colony counting. The experiment was performed in triplicate.

K. pneumoniae produces a capsular polysaccharide that may be released into the extracellular environment to form biofilms that can increase host defenses and tolerance against antimicrobials (Anderl et al., 2000). We tested the inhibition of K7 biofilm formation by phage BUCT631. Briefly, overnight grown cultures of K7 were diluted to 1:100 in fresh TSB medium, and 100 μL of the diluted culture was added to the well of a plate (Cat# 701001, Nest, China). Then, 100 μL phage was added at MOIs of 0.1, 1 and 10, respectively. Adding 100 μL fresh TSB medium was used as the control group. The plates were incubated at 37 °C for 24 h without shaking, and the biofilm was stained according to the method described previously (Li et al., 2022b). The absorbance at 595 nm was measured using a microplate reader (Synergy H1, BioTek, USA).

2.11. Phage therapy in the Galleria mellonella larvae infection model

Galleria mellonella (*G. mellonella*) larvae were used as a model to assess the therapeutic effects of the phage BUCT631 against *K. pneumoniae* strain K7. All *G. mellonella* larvae were obtained from Huiyude Biotech Company

(Tianjin, China) and were randomly selected (weight 250–300 mg). To determine the appropriate concentration of infecting bacteria, the *G. mellonella* larvae were randomly divided into 6 groups: group 1 larvae were given 5 μL of PBS, groups 2–6 larvae were injected with 5 μL of different concentrations of the bacteria (1×10^7 CFU/mL, 2×10^7 CFU/mL, 4×10^7 CFU/mL, 6×10^7 CFU/mL and 8×10^7 CFU/mL), respectively.

Bacterial concentrations of 4×10^7 CFU/mL were selected for phage treatment investigation. The larvae were randomly selected and divided into 6 groups: group I larvae were injected with 5 μL of PBS and then 5 μL of phage BUCT631 (4×10^8 PFU/mL) at 2 h post-infection (hpi), group II larvae were injected with 5 μL of K7 (4×10^7 CFU/mL) and then 5 μL of PBS, group III larvae were injected with 5 μL of K7 (4×10^7 CFU/mL) and then 5 μL of phage BUCT631 (4×10^5 PFU/mL) at 2 hpi, group IV larvae were injected with 5 μL of K7 (4×10^7 CFU/mL) and then 5 μL of phage BUCT631 (4×10^6 PFU/mL) at 2 hpi, group V larvae were injected with 5 μL of K7 (4×10^7 CFU/mL) and then 5 μL of phage BUCT631 (4×10^7 PFU/mL) at 2 hpi, group VI larvae were injected with 5 μL of K7 (4×10^7 CFU/mL) and then 5 μL of phage BUCT631 (4×10^8 PFU/mL) at 2 hpi. All experiments used 10 larvae per group and were repeated three times. The treated larvae in every group were incubated in the dark at 37 °C and evaluated for their survival every 12 h up to 120 h. The larvae were considered as dead only if they did not move when touched by a hard or sharp object. The bacterial load of the larvae in groups II, IV, V and VI was measured on LB agar by plating 0.1 mL of
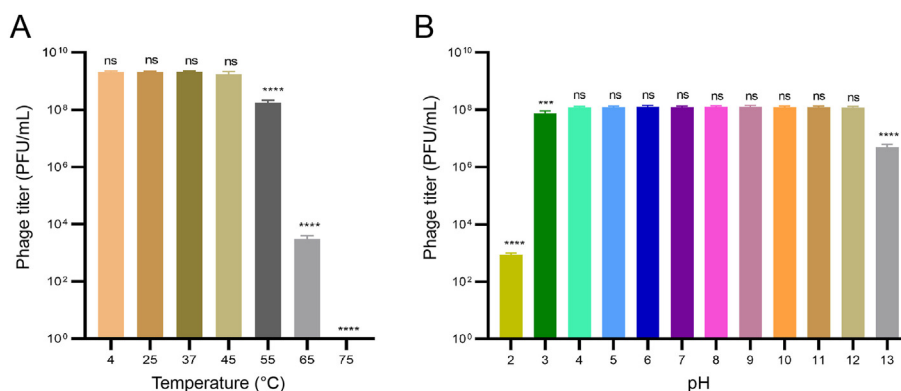

Fig. 3. Sensitivity of phage BUCT631 to temperature and pH. **A** Thermal stability of BUCT631. The purified phage BUCT631 suspensions were incubated at 4, 25, 37, 45, 55, 65 and 75 °C for 12 h, and then the phage titer was detected. **B** pH stability of BUCT631. BUCT631 suspensions were incubated at different pH levels ranging from 2 to 13 for 12 h, and then the phage titer was detected. Data are shown as the mean ± standard deviation. Statistical analysis was performed by one-way analysis of variance following a Dunnett's multiple comparisons test. ***$P < 0.001$, ****$P < 0.0001$, ns, not significant.

homogenized sample using the serial dilution method every 24 h up to 120 h.

2.12. Statistical analysis

All data were analyzed using GraphPad Prism 8.0.1 and expressed as the means and standard deviation values. One-way analysis of variance following a Dunnett's multiple comparisons test was performed. The Kaplan-Meier method with log-rank test was used to analyze *G. mellonella* larvae survival curves.

3. Results

3.1. Isolation and morphology of phage BUCT631

The phage BUCT631 was isolated from hospital sewage using clinical *K. pneumoniae* strain K7. BUCT631 formed clear and regular plaques, which were transparent in the center and had a translucent halo at the periphery, after 12 h incubation on the lawn of *K. pneumoniae* strain K7, and the diameter of plaques was approximately 5.1 ± 0.77 mm (Fig. 1A). Transmission electron microscopy (TEM) analysis showed that BUCT631 had an icosahedral head with an average diameter of 49.55 ± 2.33 nm (n = 10) and a noncontractile short tail averaging 16.39 ± 1.12 nm (n = 10) in length (Fig. 1B).

3.2. Host range

The host range plays an important role in the therapeutic application of phages. Using a panel of thirty *K. pneumoniae* strains to evaluate the host range of phage BUCT631, the result showed BUCT631 infected all tested K1 *K. pneumoniae* and failed to infect other capsular types of *K. pneumoniae* (Table 1). These results suggest that BUCT631 has strong host specificity.

3.3. Biological characterization of phage BUCT631

The phage BUCT631 was mixed with the host *K. pneumoniae* strain K7 at different MOIs, and BUCT631 when infected with *K. pneumoniae* strain K7 at an MOI of 0.01 produced a maximum titer that was significantly higher than that of the other groups (Fig. 2A), indicating that 0.01 was the optimal MOI for phage BUCT631. The adsorption curve analysis showed that more than 90% of phage BUCT631 was completely adsorbed to the host *K. pneumoniae* strain K7 after 15 min incubation (Fig. 2B). The one-step growth curve of phage BUCT631 was plotted based on the experimental data. The results showed that the latent period of phage BUCT631 was 16 min, and then the phage titer gradually increased and entered the plateau period at 90 min (Fig. 2C). The burst size of phage BUCT631, defined as the phage titer in the plateau period divided by the titer in the latent period (Lee et al., 2019), was approximately 303 ± 35 (n = 3) PFU per infected cell.

3.4. Sensitivity of phage BUCT631 to temperature and pH

The phage titer of BUCT631 had no significant change when incubated at 4−45 °C for 12 h. After incubation at 55 °C for 12 h, the phage titer decreased almost 10-fold. Subsequently, the phage titer decreased sharply with increasing temperature and dropped to 0 after incubation at 75 °C for 12 h (Fig. 3A). These data indicated that phage BUCT631 could tolerate normal temperatures and was not suitable for use at high temperatures. Phage BUCT631 showed good stability in the pH range of 4–12 for 12 h, while the phage titer was significantly reduced at pH values below 4 or above 12 (Fig. 3B). This showed that phage BUCT631 was more tolerant to alkaline environments.

Table 2
Features of the open reading frames (ORFs) of phage BUCT631.

ORF	Strand	Start	Stop	Length (AA)	Predicted Protein Function	Best-match BLASTp Result	Query cover	E-values	Identity	Accession	MW (kDa)
1	−	935	12	307	Tail fiber protein	Klebsiella phage vB_KpmP_KpV48	100%	0.0	85.85%	YP_009787605.1	33.0
2	−	4635	937	1232	Internal core protein	Klebsiella phage KpV475	100%	0.0	99.03%	YP_009280711.1	133.8
3	−	7370	4686	894	Internal virion protein B	Klebsiella phage VLCpiA1o	100%	0.0	98.55%	UVX29035.1	97.3
4	−	7975	7388	195	Internal virion protein A	Klebsiella phage KpV41	93%	1e−100	96.70%	YP_009188785.1	20.4
5	−	10,337	7977	786	Tail tubular protein B	Klebsiella phage KpV41	100%	0.0	98.85%	YP_009188784.1	86.0
6	−	10,850	10,347	167	Tail tubular protein A	Klebsiella phage F19	92%	6e−110	99.35%	YP_009006060.1	19.2
7	−	11,367	10,900	155	HNH endonuclease	Klebsiella phage VLCpiA1d	100%	9e−109	96.13%	UVX31816.1	17.6
8	−	11,636	11,454	60	Hypothetical protein	Klebsiella phage KP34	66%	2e−17	100.00%	YP_003347637.1	6.20
9	−	12,667	11,648	339	Major capsid protein	Klebsiella phage Kp_Pokalde_001	96%	0.0	100.00%	QWT56628.1	37.7
10	−	13,535	12,693	280	Scaffolding protein	Klebsiella phage vB_KpmP_KpV74	100%	0.0	97.14%	YP_009789278.1	30.1
11	−	15,145	13,550	531	Portal protein	Klebsiella phage FK1979	100%	0.0	99.44%	UPW35156.1	58.1
12	−	15,421	15,155	80	Hypothetical protein	Klebsiella phage Kpn BHU1	100%	9e−21	96.59%	UJQ45021.1	8.9
13	−	15,858	15,418	146	Hypothetical protein	Klebsiella phage SKP1	100%	6e−103	99.32%	UYE94866.1	16.4
14	−	18,352	15,884	822	DNA-dependent RNA polymerase	Klebsiella phage BUCT86	100%	0.0	98.91%	UFX84346.1	92.7
15	−	18,507	18,391	38	Hypothetical protein	Klebsiella phage vB_KpmP_KpV48	100%	2e−19	100.00%	YP_009787591.1	4.8
16	−	18,808	18,494	104	Hypothetical protein	Klebsiella phage vB_KpmP_SU552A	100%	2e−60	100.00%	YP_009204822.1	11.2
17	−	19,299	18,805	164	Polynucleotide kinase	Klebsiella phage VLCpiA1g	100%	1e−116	99.39%	UVX31778.1	18.5
18	−	19,793	19,296	165	DNA endonuclease VII	Klebsiella phage VLC5	84%	2e−80	100.00%	QIW86404.1	18.1
19	−	20,139	19,939	66	Hypothetical protein	Klebsiella virus 2019KP1	100%	5e−39	100.00%	QJT70489.1	7.7
20	−	21,064	20,096	322	5'-3' exonuclease	Klebsiella phage phiKp52	100%	0.0	99.69%	YP_009792381.1	36.6
21	−	21,222	21,064	52	Hypothetical protein	Klebsiella phage vB_KpmP_SU552A	100%	4e−20	100.00%	YP_009204817.1	5.9

Table 2 (*continued*)

ORF	Strand	Start	Stop	Length (AA)	Predicted Protein Function	Best-match BLASTp Result	Query cover	E-values	Identity	Accession	MW (kDa)
22	–	21,422	21,225	65	Hypothetical protein	*Klebsiella* phage JKP2	100%	4e−40	100.00%	UUB20331.1	7.6
23	–	21,796	21,425	123	Hypothetical protein	*Klebsiella* phage BUCT86	100%	8e−76	95.12%	UFX84337.1	13.2
24	–	21,988	21,800	62	Hypothetical protein	*Klebsiella* phage VLCpiA1a	95%	5e−08	48.39%	UVX29699.1	6.8
25	–	22,244	22,044	66	Hypothetical protein	*Klebsiella* phage KpV41	100%	2e−34	95.45%	YP_009188766.1	7.3
26	–	23,283	22,456	275	Hypothetical protein	*Klebsiella* phage BUCT86	100%	0.0	97.11%	UFX84334.1	29.2
27	–	23,496	23,335	53	Hypothetical protein	*Klebsiella* phage VLC5	66%	3e−14	100.00%	QIW86393.1	5.7
28	–	24,966	23,983	327	Phosphoesterase	*Klebsiella* phage KPR2	100%	0.0	98.47%	QCG76611.1	36.6
29	–	25,349	25,128	73	Hypothetical protein	*Klebsiella* phage VLCpiA1g	100%	2e−43	98.63%	UVX31766.1	8.1
30	–	25,887	25,339	182	Nucleotidyltransferase	*Klebsiella* phage VLCpiA1b	100%	6e−111	86.26%	UVX31205.1	21.1
31	–	28,295	25,884	803	DNA polymerase	*Klebsiella* phage KpV71	100%	0.0	98.26%	YP_009302723.1	91.9
32	–	28,474	28,292	60	Hypothetical protein	*Klebsiella* phage KpV41	100%	3e−35	100.00%	YP_009188760.1	7.0
33	–	28,620	28,465	51	Hypothetical protein	*Klebsiella* phage KpV41	100%	4e−27	98.04%	YP_009188759.1	5.8
34	–	29,953	28,673	426	DNA helicase	*Klebsiella* phage KpV41	100%	0.0	99.53%	YP_009188758.1	47.6
35	–	30,148	29,954	64	Hypothetical protein	*Klebsiella* phage vB_KpnP_IME308	100%	5e−38	100.00%	QEQ50348.1	7.0
36	–	30,930	30,145	261	DNA primase	*Klebsiella* phage KPPK108.1	100%	3e−167	98.85%	UFK09477.1	29.1
37	–	31,152	30,931	73	Hypothetical protein	*Klebsiella* phage Pone	98%	4e−17	56.94%	QPB09052.1	8.2
38	–	31,634	31,137	165	Hypothetical protein	*Klebsiella* phage KP34	96%	2e−74	73.75%	YP_003347663.1	18.3
39	–	32,683	31,637	348	Peptidase	*Klebsiella* phage VLCpiA1n	100%	0.0	97.41%	UVX29237.1	39.0
40	–	34,356	32,683	557	Hypothetical protein	*Klebsiella* phage vB_KpnP_NER40	100%	0.0	91.38%	UKS71305.1	63.3
41	–	34,747	34,403	114	Hypothetical protein	*Klebsiella* phage KpV41	100%	9e−62	92.11%	YP_009188751.1	13.5
42	–	34,953	34,735	72	Hypothetical protein	*Klebsiella* phage vB_KpnP_IME337	100%	1e−42	94.44%	QEQ50435.1	8.2
43	–	35,135	34,950	61	Hypothetical protein	*Klebsiella* phage 6993	100%	9e−34	91.80%	URY99622.1	7.1
44	–	35,371	35,132	79	Hypothetical protein	*Klebsiella* phage 1 TK-2018	92%	4e−44	97.26%	AZF88735.1	8.8
45	–	35,515	35,384	43	Hypothetical protein	*Klebsiella* phage SKP1	95%	1e−19	97.56%	UYE94836.1	4.6
46	–	35,850	35,632	72	Hypothetical protein	*Klebsiella* phage SRD2021	98%	4e−40	87.32%	QWY13494.1	8.4
47	–	36,136	35,912	74	Hypothetical protein	*Klebsiella* phage KP-Rio/2015	100%	7e−34	89.19%	YP_009787350.1	8.0
48	–	36,714	36,133	193	Hypothetical protein	*Klebsiella* phage VLCpiA1b	100%	2e−131	96.91%	UVX31242.1	20.9
49	–	38,776	38,321	151	Putative HNH endonuclease	*Klebsiella* phage BUCT86	100%	3e−93	97.35%	UFX84369.1	17.9
50	–	40,844	38,886	652	Tail spike protein	*Klebsiella* phage VLCpiA1c	100%	0.0	97.09%	UVX30914.1	70.2
51	–	41,453	40,845	202	Endolysin	*Klebsiella* phage VLCpiA1c	100%	3e−128	97.03%	UVX30915.1	21.9
52	–	41,688	41,437	83	Holin	*Klebsiella* phage vB_KpnP_SU503	100%	3e−39	100.00%	YP_009199935.1	9.2
53	–	42,085	41,681	134	Spanin	*Klebsiella* phage vB_KpP-Screen	100%	2e−62	98.51%	CAD5239038.1	14.0
54	–	42,267	42,085	60	Hypothetical protein	*Klebsiella* phage CX1	76%	4e−23	100.00%	QIN95028.1	6.2
55	–	42,653	42,279	124	Hypothetical protein	*Klebsiella* phage myPSH1235	100%	1e−82	100.00%	YP_009799492.1	13.0
56	–	44,509	42,653	618	Terminase large subunit	*Klebsiella* phage BUCT86	100%	0.0	99.51%	UFX84362.1	69.5
57	–	44,811	44,509	100	Terminase small subunit	*Klebsiella* phage VLCpiA1r	100%	3e−61	99.00%	UVX29053.1	11.3

3.5. Genomic characterization of the phage BUCT631

The genome of phage BUCT631 is double-stranded DNA with a total length of 44,812 bp and a G + C content of 54.1%. Analysis of the genome by bioinformatics software revealed that the genome of BUCT631 encodes a total of 57 ORFs, and no tRNA genes, known drug resistance genes or virulence factor genes were found. Annotation by BLASTp showed that only 27 of the 57 ORFs encoded by the BUCT631 genome were annotated as functional proteins, and the rest of the ORFs were annotated as hypothetical proteins (Table 2).

The visualization of functional proteins in the phage BUCT631 genome is shown in Fig. 4, which involves mainly five functional modules, including: phage lysis, packing, regulation, replication and structure. Analysis of the whole genome of phage BUCT631 found that ORF50 encoded the tail spike protein, which was located in the same gene cluster as the phage lysozyme-related genes. The tail spike proteins of phages usually exhibit depolymerase activity and form a halo around the phage plaque center (Domingo-Calap et al., 2020). ORF50 was analyzed and found to have the amino acid and structural homology with depolymerase in protein databases (PDB: 7W1E) by using HHpred (Söding et al., 2005). Therefore, we hypothesize that the tail spike protein of BUCT631 has depolymerase activity.

Except for the ORFs annotated to function, an additional 30 ORFs in the BUCT631 genome were predicted to be hypothetical proteins. The conserved domains of these hypothetical proteins were searched using CD-Search, and the results showed that ORF15, ORF16, ORF26, ORF27 and ORF44 have conserved domains, but their functions are unknown (Supplementary Table S2). In addition, these hypothetical proteins were predicted using PhANNs (Cantu et al., 2020), and ORF12 was found to be associated with tail fiber, ORF29 with portal, and ORF55 with minor capsid (Supplementary Table S3). The accuracy of hypothetical proteins needs to be verified in further research.

3.6. Evolutionary analysis of the phage BUCT631

To determine the evolutionary relationships between phage BUCT631 and other phages, a phylogenetic tree was constructed using the evolutionarily significant and conserved phage major capsid protein (ORF9), DNA polymerase (ORF31) and terminase large subunit (ORF56). The major capsid protein analysis revealed a high correlation between BUCT631 and *Klebsiella* phage P929 (GenBank ID: OK562429.1) (Fig. 5A). The DNA polymerase analysis showed a high correlation between BUCT631 and *Klebsiella* phage vB_KpnP_KpV74 (GenBank ID: NC_047811.1) (Fig. 5B). In addition, the terminase large subunit analysis showed a high correlation between BUCT631 and Klebsiella phage VLCpiA1d (GenBank ID: ON602762.1) (Fig. 5C). Furthermore, inter-genomic similarity calculations using VIRIDIC revealed a maximum similarity of 84.7% between BUCT631 and *Klebsiella* phage vB_KpnP_KpV475 (GenBank ID: NC_031025.1) (Fig. 5D). These phages all belong to the genus *Drulisvirus* of the subfamily *Slopekvirinae* in the family *Autographiviridae*, so we propose that phage BUCT631 should be classified as a new species in the genus *Drulisvirus*.

3.7. Evaluation of phage BUCT631 against K. pneumoniae strain K7 in vitro and in vivo

Characterization of phage lytic activity *in vitro* is the first step for assessing the efficacy of phage therapy. In this study, the phage BUCT631 was mixed with *K. pneumoniae* strain K7 in pre-logarithmic growth phase at different MOIs and co-incubated for 12 h. The results showed that the growth of K7 cells treated with phage BUCT631 at MOIs of 0.01, 0.1, 1, 10 and 100 was completely inhibited after 2 h of co-culture, which could last for 6 h (Fig. 6A). Subsequently, the OD_{600} of each group cultures gradually increased, which may be due to a few bacteria escaping from phage killing or developing phage-resistant strains. In addition, there was a significant difference in the bacterial count between the treatment
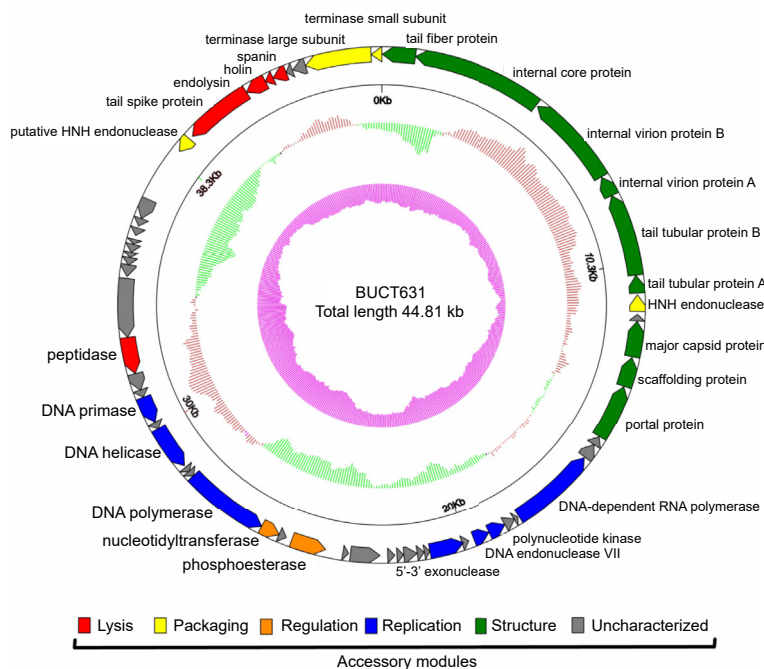

Fig. 4. Genome map of phage BUCT631. ORFs are represented in different colors according to their functional categories. Red: lysis-related proteins; yellow: packaging-related proteins; orange: regulation-related proteins; blue: replication-related proteins; green: structure-related proteins; gray: uncharacterized proteins. The innermost purple circles represent G + C skew of G − C/G + C (inward represents less than 0). Secondary inner circle represents the (G + C) mol%, and red indicates that the content is greater than the whole genome average (G + C) mol%, and green indicates that the content is lower than the average (G + C) mol%.

group and the control group at each time interval and MOI (Fig. 6B). Overall, the phage BUCT631 can effectively inhibit the growth of K7 *in vitro*.

The ability of phages to inhibit bacterial biofilm formation can be considered an advantage. A significant difference ($P < 0.0001$) was observed in the attached biomass of *K. pneumoniae* K7 treated with phage BUCT631 at different MOIs (0.1, 1, 10) when assessed by the crystal violet assay (Fig. 6C). These results indicated that phage BUCT631 could significantly inhibit biofilm formation of *K. pneumoniae* K7.

Given the remarkable similarity of their innate immune response to that of vertebrates, *G. mellonella* have been widely used as an alternative model for evaluating the virulence of microbial pathogens and the effectiveness of antimicrobial substances *in vivo* (Ménard et al., 2021). In this study, we evaluated the effect of phage treatment in *G. mellonella* Larvae model, and the experimental flow is shown in Fig. 7A.

G. mellonella were injected with different concentrations of *K. pneumoniae* strain K7 to establish the infection model. The results showed that injection of 5 μL of K7 at a concentration of 2×10^7 CFU/mL resulted in 50% death of *G. mellonella* (Fig. 7B). K7 (4×10^7 CFU/mL), higher than half lethal bacterial concentration, was selected for *G. mellonella* infection, followed by injection of phage BUCT631 with different MOIs for phage treatment evaluation. The survival rates of *G. mellonella* treated with phage BUCT631 at MOIs of 0.01, 0.1, 1 and 10 were improved by 20%, 40%, 70% and 80%, respectively, compared to the group that was not treated with phage BUCT631 (Fig. 7C). The morphology of *G. mellonella* in each group is shown in Supplementary Fig. S1. In addition, the number of bacteria in *G. mellonella* larvae was significantly reduced in the phage treatment group (Fig. 7D). Although the bacteria in the phage treatment group were not eliminated, this phenomenon may be beneficial because this low load of bacteria has the opportunity to
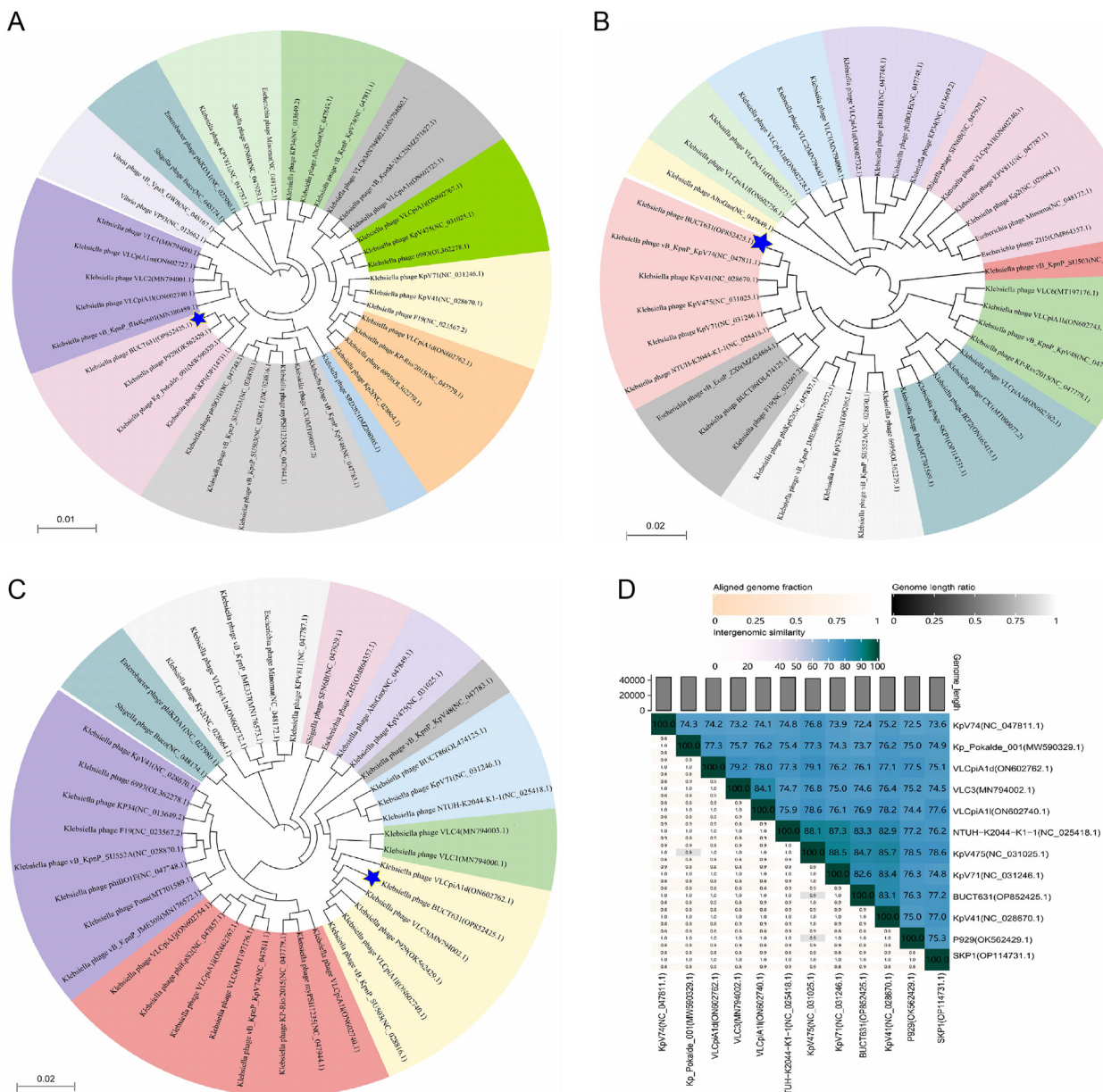

Fig. 5. Phylogenetic analysis of phage BUCT631. The phylogenetic tree was constructed based on the amino acid sequences of the major capsid (**A**), DNA polymerase (**B**) and terminase large subunit (**C**) using the neighbor-joining method with 1000 bootstrap replicates in MEGA 7. The amino acid sequences of the related phages were downloaded from NCBI. Phage BUCT631 is labeled with a blue triangle. Phages located in a co-evolutionary cluster are marked with the same color. **D** Percentage sequence similarity between phage BUCT631 genome and phages of genus Drulisvirus genomes. The values were calculated using VIDIRIC. The horizontal and vertical coordinates indicate the corresponding phage and Genebank number.
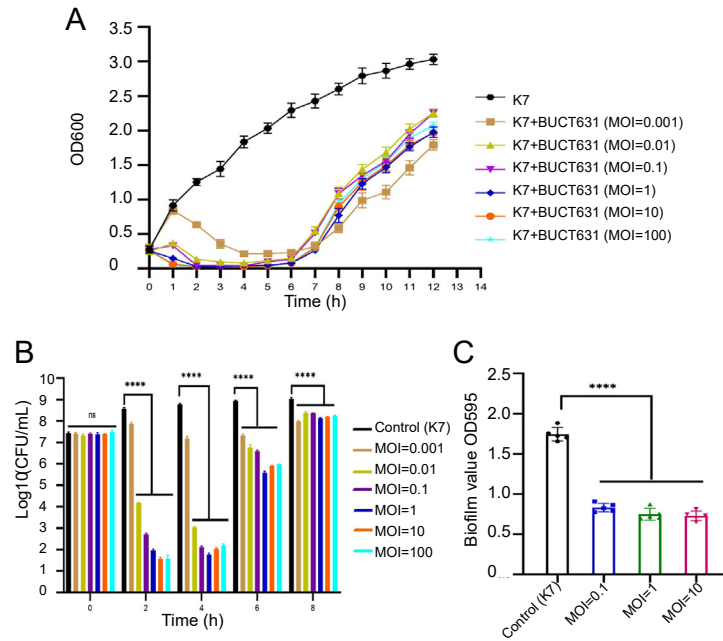
Fig. 6. Assessment the efficacy of phage BUCT631 against *K. pneumoniae* strain K7 *in vitro*. **A** Inhibition of K7 growth by BUCT631. K7 was co-cultivated with BUCT631 at different MOIs at 37 °C with shaking for 12 h, and the absorbance (OD$_{600}$) of each group was measured every 1 h. **B** Changes in bacterial loads during co-culture. Samples were taken from different MOIs mixtures every 2 h for colony counting using the serial dilution method. **C** The biofilm inhibition effect of phage BUCT631. K7 was co-incubated with BUCT631 at an MOI of 0.1, 1 and 10 for 24 h at 37 °C. After incubation, biofilm formed of K7 was measured by CV assay (absorbance at 595 nm). Data are shown as the mean ± standard deviatioin. Statistical analysis was performed by one-way analysis of variance following a Dunnett's multiple comparisons test. ****$P < 0.0001$, ns, not significant.
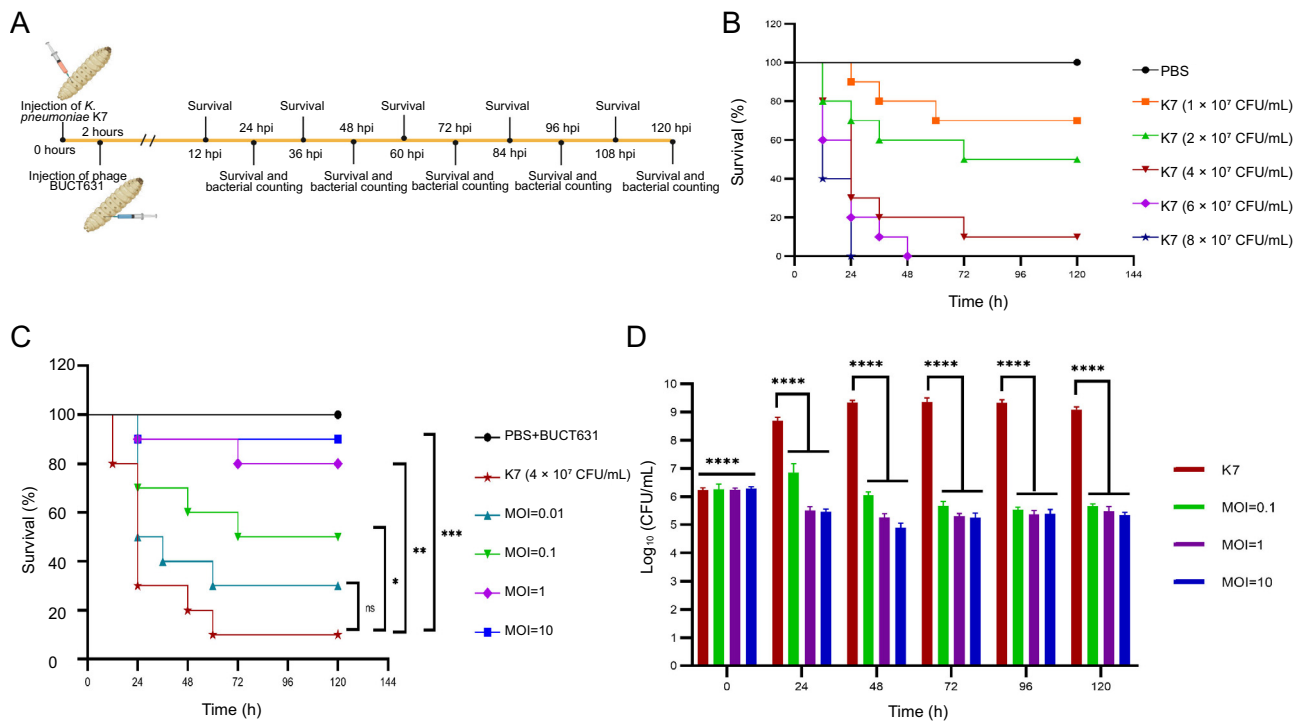

Fig. 7. Phage therapy in the *G. mellonella* model. **A** Schematic representation of phage BUCT631 treating *K. pneumoniae* K7-infected *G. mellonella*. HPI: hours post inoculation. **B** Survival curves of *G. mellonella* infected with K7 or PBS. The *G. mellonella* larvae were injected with 5 μL of different concentrations of K7 or PBS, and then incubated at 37 °C and evaluated for their survival every 12 h up to 120 h. **C** Survival curves of *G. mellonella* infected with K7 followed by phage treatment. The *G. mellonella* larvae were injected with 5 μL of K7 (4×10^7 CFU/mL) and then injected with BUCT631 at different MOIs. Survival counts as described above. **D** Changes in bacterial loads in phage treatment. The *G. mellonella* larvae infected with K7 were treated with BUCT631 at an MOI of 0.1, 1, and 10. After treatment for 24, 48, 72, 96 and 120 h, the bacteria loads were determined using the serial dilution method. Data represent the mean ± standard deviation. The data in Fig. 7C were statistically analyzed using the Kaplan-Meier method with log-rank test. The data in Fig. 7D were statistically analyzed using one-way analysis of variance following a Dunnett's multiple comparisons test. *$P < 0.05$; **$P < 0.01$; ***$P < 0.001$; ****$P < 0.0001$; ns, not significant.

enhance the immunity of *G. mellonella*. The above results suggest that phage BUCT631 can effectively treat K7 infection *in vivo*.

4. Discussion

Phages are the most abundant and diverse species in the biosphere, which makes different ecological environments an important source of phages. Targeting hospital-acquired pathogens, hospital sewage provides a resource for phage isolation against drug-resistant bacteria (Feng et al., 2023; Han et al., 2021). Phage-bacteria interactions in the environment are complex, and phages only recognize specific bacteria and kill them. For the widespread use of phages, efforts should be made to isolate more phages with different host ranges, and the isolation of new phages capable of targeting specific epidemic strains is essential for the clinical application of phages. In this study, we isolated and identified phage BUCT631 from hospital sewage, which can specifically lyse drug-resistant K1 *K. pneumoniae* and could potentially be used as a tool for the treatment of antibiotic-ineffective K1 *K. pneumoniae* infections.

In most hvKp strains, the levels of capsule production are increased to protect the bacteria from harmful irritants, and this hypermucoviscous phenotype has most often been observed in K1 *K. pneumoniae* strains. As natural enemies of bacteria, phages produce "capsule depolymerase" for enzymatic degradation to break through this protective barrier (Latka et al., 2017). A translucent halo was formed around the plaques, indicating that phage BUC631 may form depolymerases with the function of removing bacterial capsular polysaccharides in the process of bacterial lysis. The tail fiber or tail spike proteins of phages usually exhibit depolymerase activity (Domingo-Calap et al., 2020). Analysis of the whole genome of phage BUCT631 found that ORF01 encoded the tail fiber protein (GP1) and ORF50 encoded the tail spike protein (GP50). GP1 was predicted to contain a phage T7 tail domain (E value = 6.93e−14) using CD-Search, and GP50 contains a beta helix domain (E value = 8.06e−03) that shares some similarity with pectate lyases (EC 4.2.2.2). From the results of amino acid similarity analysis, GP50 is likely exhibits polysaccharide-degrading activity, which requires protein expression and activity verification in the future. Previous studies have shown that depolymerases have advantages of high stability, strong specificity and efficient inhibition of biofilm formation (Pires et al., 2016). Further in-depth studies on phage BUCT631 depolymerase will help to expand the application of phage BUCT631 in the future.

Lytic bacteriophages are considered as the most accessible and acceptable alternative to antibiotics against *K. pneumoniae* infections (Hung et al., 2011). At present, many phages capable of lysing K1 *K. pneumoniae* have been reported, representative of which are KpV41, KpV475, KpV71, vB_KpnP_K1-ULIP33 and NTUH-K2044-K1-1 (Lin et al., 2014; Solovieva et al., 2018; Thiry et al., 2019), but these phages have not been studied for growth characteristics. The latent period and burst size of phages have been observed in laboratory studies as one of the characteristics of their high lytic activity (Rohde et al., 2018). One-step growth curve is an experimental curve used to quantitatively describe the growth pattern of phages. The results of this study showed that phage BUCT631 had a latent period of 16 min and a burst size of approximately 303 PFU/cell (Fig. 2C), which is superior to K1 *K. pneumoniae* phage Henu1 (latent period of 30 min and burst size of 95 PFU/cell) (Teng et al., 2019), indicating that phage BUCT631 has a strong lysis property. In addition, the thermal and pH stability showed that phage BUCT631 had good temperature (4–50 °C) and pH (pH = 4–12) tolerance (Fig. 3), which was similar to that previously reported for *Klebsiella pneumoniae* phages P929 and P13 (Chen et al., 2022; Fang and Zong, 2022). The safety of phages for phage therapy can be predicted by bioinformatics analysis. Notably, no virulence or antibiotic resistance related genes were annotated in the genome of phage BUCT631, suggesting that using BUCT631 as a therapeutic or biological control agent is safe.

Evaluation of phages for the treatment of bacterial-induced infections in animal infection models is an important reference for the clinical application of phages. Compared to other animals, *G.mellonella* has been widely used as a model of bacterial infection due to its advantages of simple operation, low cost, short life cycle and fewer ethical problems. Therefore, we evaluated the effectiveness of phage treatment using the *G. mellonella* infection model in this study. The results showed that phage BUCT631 with different MOIs improved the survival of K1 *K. pneumoniae* infected *G. mellonella* larvae (Fig. 7C). Moreover, the survival rate increased by 80% upon treatment with phage BUCT631 at an MOI of 10, which was superior to the efficacy of *K. pneumoniae* phages vB_KpnP_K1-ULIP33 and vB_KpnS_SXFY507 in a *G. mellonella* infection model (Feng et al., 2023; Thiry et al., 2019). These results suggest that phage BUCT631 has potential for clinical application as a therapeutic agent.

Although phage BUCT631 was able to completely inhibit the growth of K1 *K. pneumoniae* within 2 h, this inhibition lasted for only 4 h until the resistant mutant was produced (Fig. 6A). Phage-resistant mutants do appear when a single phage is used to treat bacteria *in vitro* and *in vivo*, which is a major limitation in phage therapeutic applications and a deficiency of our study. To overcome the problem of phage resistance, phage therapy usually uses phage cocktails. Mixing phages with different host ranges into cocktails not only expands the antimicrobial spectrum activity, but also inhibits the emergence of phage-resistant bacterial mutants (Gu et al., 2012). Accelerating the isolation and identification of novel phages and genome sequencing research to clarify the interaction mechanism between phages and host bacteria are of great significance to the future development of phage therapy.

5. Conclusions

In this study, phage BUCT631 with strong lytic activity against drug-resistant *K. pneumoniae* was characterized in depth. Overall, the phage BUCT631 has a large burst size, short latent period and high adsorption rate, which are among the phage traits contributing to its high virulence (relative ability to lyse host bacterial cells), and has shown potential to treat multidrug-resistant K1 *K. pneumoniae* infections *in vitro* and *in vivo*. Thus, our study not only enriches the knowledge of *K. pneumoniae* phages, but also provides a novel resource for the development of phage therapy against multidrug-resistant K1 *K. pneumoniae*.

Data availability

The complete genome sequence of phage BUCT631 has been deposited in GenBank under the accession number OP852425.

Ethics statement

The study was approved by the Ethics Committee of Chinese PLA Army General Hospital. All procedures were conducted following the according guidelines.

Author contributions

Pengjun Han: conceptualization, investigation, methodology, validation, writing original draft, writing-review and editing. Mingfang Pu: validation. Yahao Li: formal analysis. Huahao Fan: supervision, funding acquisition, writing-review and editing. Yigang Tong: resources, project administration, funding acquisition.

Conflict of interest

Prof. Yigang Tong is an Editorial Board member for *Virologica Sinica* and was not involved in the editorial review or the decision to publish this article. All the authors declare no competing interests.

Acknowledgements

supported by the National Key Research and Development Program of China (NO. 2018YFA0903000, 2020YFC2005405, 2020YFA0712100, 2020YFC0840805), the Funds for First-class Discipline Construction (NO. XK1805, NO. XK1803-06) and the Innovation & Transfer Fund of Peking University Third Hospital BYSYZHKC2022114.

Appendix A. Supplementary data

Supplementary data to this article can be found online at https://doi.org/10.1016/j.virs.2023.07.002.

References

Altschul, S.F., Madden, T.L., Schäffer, A.A., Zhang, J., Zhang, Z., Miller, W., Lipman, D.J., 1997. Gapped BLAST and PSI-BLAST: a new generation of protein database search programs. Nucleic Acids Res. 25, 3389–3402.

Anderl, J.N., Franklin, M.J., Stewart, P.S., 2000. Role of antibiotic penetration limitation in Klebsiella pneumoniae biofilm resistance to ampicillin and ciprofloxacin. Antimicrob. Agents Chemother. 44, 1818–1824.

Bankevich, A., Nurk, S., Antipov, D., Gurevich, A.A., Dvorkin, M., Kulikov, A.S., Lesin, V.M., Nikolenko, S.I., Pham, S., Prjibelski, A.D., Pyshkin, A.V., Sirotkin, A.V., Vyahhi, N., Tesler, G., Alekseyev, M.A., Pevzner, P.A., 2012. SPAdes: a new genome assembly algorithm and its applications to single-cell sequencing. J. Comput. Biol. 19, 455–477.

Bao, J., Wu, N., Zeng, Y., Chen, L., Li, L., Yang, L., Zhang, Y., Guo, M., Li, L., Li, J., Tan, D., Cheng, M., Gu, J., Qin, J., Liu, J., Li, S., Pan, G., Jin, X., Yao, B., Guo, X., Zhu, T., Le, S., 2020. Non-active antibiotic and bacteriophage synergism to successfully treat recurrent urinary tract infection caused by extensively drug-resistant Klebsiella pneumoniae. Emerg. Microb. Infect. 9, 771–774.

Bengoechea, J.A., Sa Pessoa, J., 2019. Klebsiella pneumoniae infection biology: living to counteract host defences. FEMS Microbiol. Rev. 43, 123–144.

Bolger, A.M., Lohse, M., Usadel, B., 2014. Trimmomatic: a flexible trimmer for Illumina sequence data. Bioinformatics 30, 2114–2120.

Cano, E.J., Caflisch, K.M., Bollyky, P.L., Van Belleghem, J.D., Patel, R., Fackler, J., Brownstein, M.J., Horne, B., Biswas, B., Henry, M., Malagon, F., Lewallen, D.G., Suh, G.A., 2021. Phage therapy for limb-threatening prosthetic knee Klebsiella pneumoniae infection: case report and in vitro characterization of anti-biofilm activity. Clin. Infect. Dis. 73, e144–e151.

Cantu, V.A., Salamon, P., Seguritan, V., Redfield, J., Salamon, D., Edwards, R.A., Segall, A.M., 2020. PhANNs, a fast and accurate tool and web server to classify phage structural proteins. PLoS Comput. Biol. 16, e1007845.

Chen, X., Tang, Q., Li, X., Zheng, X., Li, P., Li, M., Wu, F., Xu, Z., Lu, R., Zhang, W., 2022. Isolation, characterization, and genome analysis of bacteriophage P929 that could specifically lyase the KL19 capsular type of Klebsiella pneumoniae. Virus Res. 314, 198750.

Choby, J.E., Howard-Anderson, J., Weiss, D.S., 2020. Hypervirulent Klebsiella pneumoniae - clinical and molecular perspectives. J. Intern. Med. 287, 283–300.

Chuang, Y.P., Fang, C.T., Lai, S.Y., Chang, S.C., Wang, J.T., 2006. Genetic determinants of capsular serotype K1 of Klebsiella pneumoniae causing primary pyogenic liver abscess. J. Infect. Dis. 193, 645–654.

Clausen, P., Aarestrup, F.M., Lund, O., 2018. Rapid and precise alignment of raw reads against redundant databases with KMA. BMC Bioinf. 19, 307.

Cosentino, S., Voldby Larsen, M., Møller Aarestrup, F., Lund, O., 2013. PathogenFinder–distinguishing friend from foe using bacterial whole genome sequence data. PLoS One 8, e77302.

Domingo-Calap, P., Beamud, B., Mora-Quilis, L., González-Candelas, F., Sanjuán, R., 2020. Isolation and characterization of two Klebsiella pneumoniae phages encoding divergent depolymerases. Int. J. Mol. Sci. 21, 3160.

Fang, C.T., Lai, S.Y., Yi, W.C., Hsueh, P.R., Liu, K.L., Chang, S.C., 2007. Klebsiella pneumoniae genotype K1: an emerging pathogen that causes septic ocular or central nervous system complications from pyogenic liver abscess. Clin. Infect. Dis. 45, 284–293.

Fang, Q., Zong, Z., 2022. Lytic phages against ST11 K47 carbapenem-resistant Klebsiella pneumoniae and the corresponding phage resistance mechanisms. mSphere 7, e0008022.

Feng, J., Li, F., Sun, L., Dong, L., Gao, L., Wang, H., Yan, L., Wu, C., 2023. Characterization and genome analysis of phage vB_KpnS_SXFY507 against Klebsiella pneumoniae and efficacy assessment in Galleria mellonella larvae. Front. Microbiol. 14, 1081715.

Gu, J., Liu, X., Li, Y., Han, W., Lei, L., Yang, Y., Zhao, H., Gao, Y., Song, J., Lu, R., Sun, C., Feng, X., 2012. A method for generation phage cocktail with great therapeutic potential. PLoS One 7, e31698.

Han, P., Hu, Y., An, X., Song, L., Fan, H., Tong, Y., 2021. Biochemical and genomic characterization of a novel bacteriophage BUCT555 lysing Stenotrophomonas maltophilia. Virus Res. 301, 198465.

Han, P., Zhang, W., Pu, M., Li, Y., Song, L., An, X., Li, M., Li, F., Zhang, S., Fan, H., Tong, Y., 2022. Characterization of the bacteriophage BUCT603 and therapeutic potential evaluation against drug-resistant stenotrophomonas maltophilia in a mouse model. Front. Microbiol. 13, 906961.

Harada, S., Ishii, Y., Saga, T., Aoki, K., Tateda, K., 2018. Molecular epidemiology of Klebsiella pneumoniae K1 and K2 isolates in Japan. Diagn. Microbiol. Infect. Dis. 91, 354–359.

Hatfull, G.F., Dedrick, R.M., Schooley, R.T., 2022. Phage therapy for antibiotic-resistant bacterial infections. Annu. Rev. Med. 73, 197–211.

Herridge, W.P., Shibu, P., O'Shea, J., Brook, T.C., Hoyles, L., 2020. Bacteriophages of Klebsiella spp., their diversity and potential therapeutic uses. J. Med. Microbiol. 69, 176–194.

Holst Sørensen, M.C., van Alphen, L.B., Fodor, C., Crowley, S.M., Christensen, B.B., Szymanski, C.M., Brøndsted, L., 2012. Phase variable expression of capsular polysaccharide modifications allows Campylobacter jejuni to avoid bacteriophage infection in chickens. Front. Cell. Infect. Microbiol. 2, 11.

Hung, C.H., Kuo, C.F., Wang, C.H., Wu, C.M., Tsao, N., 2011. Experimental phage therapy in treating Klebsiella pneumoniae-mediated liver abscesses and bacteremia in mice. Antimicrob. Agents Chemother. 55, 1358–1365.

Kim, S.G., Lee, S.B., Giri, S.S., Kim, H.J., Kim, S.W., Kwon, J., Park, J., Roh, E., Park, S.C., 2020. Characterization of novel erwinia amylovora jumbo bacteriophages from eneladusvirus genus. Viruses 12, 1373.

Kumar, S., Stecher, G., Tamura, K., 2016. MEGA7: molecular evolutionary genetics analysis version 7.0 for bigger datasets. Mol. Biol. Evol. 33, 1870–1874.

Latka, A., Maciejewska, B., Majkowska-Skrobek, G., Briers, Y., Drulis-Kawa, Z., 2017. Bacteriophage-encoded virion-associated enzymes to overcome the carbohydrate barriers during the infection process. Appl. Microbiol. Biotechnol. 101, 3103–3119.

Lee, D., Im, J., Na, H., Ryu, S., Yun, C.H., Han, S.H., 2019. The novel Enterococcus phage vB_EfaS_HEf13 has broad lytic activity against clinical isolates of Enterococcus faecalis. Front. Microbiol. 10, 2877.

Letarov, A.V., Kulikov, E.E., 2017. Adsorption of bacteriophages on bacterial cells. Biochemistry (Mosc.) 82, 1632–1658.

Li, L., Zhang, Z., 2014. Isolation and characterization of a virulent bacteriophage SPW specific for Staphylococcus aureus isolated from bovine mastitis of lactating dairy cattle. Mol. Biol. Rep. 41, 5829–5838.

Li, M., Wang, H., Chen, L., Guo, G., Li, P., Ma, J., Chen, R., Du, H., Liu, Y., Zhang, W., 2022a. Identification of a phage-derived depolymerase specific for KL47 capsule of Klebsiella pneumoniae and its therapeutic potential in mice. Virol. Sin. 37, 538–546.

Li, P., Ma, W., Shen, J., Zhou, X., 2022b. Characterization of novel bacteriophage vB_KpnP_ZX1 and its depolymerases with therapeutic potential for K57 Klebsiella pneumoniae infection. Pharmaceutics 14, 1916.

Lin, T.L., Hsieh, P.F., Huang, Y.T., Lee, W.C., Tsai, Y.T., Su, P.A., Pan, Y.J., Hsu, C.R., Wu, M.C., Wang, J.T., 2014. Isolation of a bacteriophage and its depolymerase specific for K1 capsule of Klebsiella pneumoniae: implication in typing and treatment. J. Infect. Dis. 210, 1734–1744.

Lin, Y.T., Cheng, Y.H., Juan, C.H., Wu, P.F., Huang, Y.W., Chou, S.H., Yang, T.C., Wang, F.D., 2018. High mortality among patients infected with hypervirulent antimicrobial-resistant capsular type K1 Klebsiella pneumoniae strains in Taiwan. Int. J. Antimicrob. Agents 52, 251–257.

Lowe, T.M., Eddy, S.R., 1997. tRNAscan-SE: a program for improved detection of transfer RNA genes in genomic sequence. Nucleic Acids Res. 25, 955–964.

Luong, T., Salabarria, A.C., Roach, D.R., 2020. Phage therapy in the resistance era: where do we stand and where are we going. Clin. Therapeut. 42, 1659–1680.

Marchler-Bauer, A., Lu, S., Anderson, J.B., Chitsaz, F., Derbyshire, M.K., DeWeese-Scott, C., Fong, J.H., Geer, L.Y., Geer, R.C., Gonzales, N.R., Gwadz, M., Hurwitz, D.I., Jackson, J.D., Ke, Z., Lanczycki, C.J., Lu, F., Marchler, G.H., Mullokandov, M., Omelchenko, M.V., Robertson, C.L., Song, J.S., Thanki, N., Yamashita, R.A., Zhang, D., Zhang, N., Zheng, C., Bryant, S.H., 2011. CDD: a Conserved Domain Database for the functional annotation of proteins. Nucleic Acids Res. 39, D225–D229.

McCallin, S., Alam Sarker, S., Barretto, C., Sultana, S., Berger, B., Huq, S., Krause, L., Bibiloni, R., Schmitt, B., Reuteler, G., Brüssow, H., 2013. Safety analysis of a Russian phage cocktail: from metagenomic analysis to oral application in healthy human subjects. Virology 443, 187–196.

McNair, K., Zhou, C., Dinsdale, E.A., Souza, B., Edwards, R.A., 2019. PHANOTATE: a novel approach to gene identification in phage genomes. Bioinformatics 35, 4537–4542.

Melo, L., Oliveira, H., Pires, D.P., Dabrowska, K., Azeredo, J., 2020. Phage therapy efficacy: a review of the last 10 years of preclinical studies. Crit. Rev. Microbiol. 46, 78–99.

Moraru, C., Varsani, A., Kropinski, A.M., 2020. VIRIDIC-A novel tool to calculate the intergenomic similarities of prokaryote-infecting viruses. Viruses 12, 1268.

Ménard, G., Rouillon, A., Cattoir, V., Donnio, P.Y., 2021. Galleria mellonella as a suitable model of bacterial infection: past, present and future. Front. Cell. Infect. Microbiol. 11, 782733.

Pires, D.P., Oliveira, H., Melo, L.D., Sillankorva, S., Azeredo, J., 2016. Bacteriophage-encoded depolymerases: their diversity and biotechnological applications. Appl. Microbiol. Biotechnol. 100, 2141–2151.

Podschun, R., Ullmann, U., 1998. Klebsiella spp. as nosocomial pathogens: epidemiology, taxonomy, typing methods, and pathogenicity factors. Clin. Microbiol. Rev. 11, 589–603.

Pu, M., Li, Y., Han, P., Lin, W., Geng, R., Qu, F., An, X., Song, L., Tong, Y., Zhang, S., Cai, Z., Fan, H., 2022. Genomic characterization of a new phage BUCT541 against Klebsiella pneumoniae K1-ST23 and efficacy assessment in mouse and Galleria mellonella larvae. Front. Microbiol. 13, 950737.

Ramirez, M.S., Traglia, G.M., Lin, D.L., Tran, T., Tolmasky, M.E., 2014. Plasmid-Mediated antibiotic resistance and virulence in gram-negatives: the Klebsiella pneumoniae paradigm. Microbiol. Spectr. 2, PLAS-0016-2013.

Rohde, C., Resch, G., Pirnay, J.P., Blasdel, B.G., Debarbieux, L., Gelman, D., Górski, A., Hazan, R., Huys, I., Kakabadze, E., Łobocka, M., Maestri, A., Almeida, G., Makalatia, K., Malik, D.J., Maślaňová, I., Merabishvili, M., Pantucek, R., Rose, T., Štveráková, D., Van Raemdonck, H., Verbeken, G., Chanishvili, N., 2018. Expert

opinion on three phage therapy related topics: bacterial phage resistance, phage training and prophages in bacterial production strains. Viruses 10, 178.

Saha, D., Mukherjee, R., 2019. Ameliorating the antimicrobial resistance crisis: phage therapy. IUBMB Life 71, 781–790.

Sarker, S.A., McCallin, S., Barretto, C., Berger, B., Pittet, A.C., Sultana, S., Krause, L., Huq, S., Bibiloni, R., Bruttin, A., Reuteler, G., Brüssow, H., 2012. Oral T4-like phage cocktail application to healthy adult volunteers from Bangladesh. Virology 434, 222–232.

Solovieva, E.V., Myakinina, V.P., Kislichkina, A.A., Krasilnikova, V.M., Verevkin, V.V., Mochalov, V.V., Lev, A.I., Fursova, N.K., Volozhantsev, N.V., 2018. Comparative genome analysis of novel Podoviruses lytic for hypermucoviscous Klebsiella pneumoniae of K1, K2, and K57 capsular types. Virus Res. 243, 10–18.

Storms, Z.J., Sauvageau, D., 2014. Evidence that the heterogeneity of a T4 population is the result of heritable traits. PLoS One 9, e116235.

Söding, J., Biegert, A., Lupas, A.N., 2005. The HHpred interactive server for protein homology detection and structure prediction. Nucleic Acids Res. 33, W244–W248.

Teng, T., Li, Q., Liu, Z., Li, X., Liu, Z., Liu, H., Liu, F., Xie, L., Wang, H., Zhang, L., Wu, D., Chen, M., Li, Y., Ji, A., 2019. Characterization and genome analysis of novel

Klebsiella phage Henu1 with lytic activity against clinical strains of Klebsiella pneumoniae. Arch. Virol. 164, 2389–2393.

Thapa, S., Adhikari, N., Shah, A.K., Lamichhane, I., Dhungel, B., Shrestha, U.T., Adhikari, B., Banjara, M.R., Ghimire, P., Rijal, K.R., 2021. Detection of NDM-1 and VIM genes in carbapenem-resistant Klebsiella pneumoniae isolates from a tertiary health-care center in kathmandu, Nepal. Chemotherapy 66, 199–209.

Thiry, D., Passet, V., Danis-Wlodarczyk, K., Lood, C., Wagemans, J., De Sordi, L., van Noort, V., Dufour, N., Debarbieux, L., Mainil, J.G., Brisse, S., Lavigne, R., 2019. New bacteriophages against emerging lineages ST23 and ST258 of Klebsiella pneumoniae and efficacy assessment in Galleria mellonella larvae. Viruses 11, 411.

Wilkins, M.R., Gasteiger, E., Bairoch, A., Sanchez, J.C., Williams, K.L., Appel, R.D., Hochstrasser, D.F., 1999. Protein identification and analysis tools in the ExPASy server. Methods Mol. Biol. 112, 531–552.

Wittebole, X., De Roock, S., Opal, S.M., 2014. A historical overview of bacteriophage therapy as an alternative to antibiotics for the treatment of bacterial pathogens. Virulence 5, 226–235.

Zhang, R., Lin, D., Chan, E.W., Gu, D., Chen, G.X., Chen, S., 2016. Emergence of carbapenem-resistant serotype K1 hypervirulent Klebsiella pneumoniae strains in China. Antimicrob. Agents Chemother. 60, 709–711.